JOURNAL OF GEOPHYSICAL RESEARCH, VOL. 105, NO. D23, PAGES 29,023–29,038, DECEMBER 16, 2000

Lamination and polar vortex development in fall from ATMOS long-lived trace gases observed during November 1994

G. L. Manney,[1,2] H. A. Michelsen,[3] F. W. Irion,[1] G. C. Toon,[1] M. R. Gunson,[1] and A. E. Roche[4]

Abstract. Long-lived trace-gas profiles observed by the Atmospheric Trace Molecule Spectroscopy (ATMOS) instrument around the developing polar vortex (the "protovortex") during early November 1994 show distinctive inversions (laminae). High-resolution profiles calculated using a reverse trajectory (RT) model reproduce the majority of these laminae, demonstrating that most of these features arise from advection by the large-scale winds. The relationship between CH_4 and N_2O sampled in filaments of low-latitude air changes from the canonical midlatitude correlation to one typical of tropical air, confirming the identification of tropical laminae. N_2O/CH_4 correlations for laminae in vortex filaments indicate that enough confined descent and mixing has already occurred in the middle and upper stratosphere by early November to alter the tracer relationship in the protovortex from that in midlatitudes. Distributions of laminae in ATMOS observations agree with regions of greater or less filamentation seen in high-resolution RT maps. There is a deep minimum in laminae occurrence between 30° and 90°E at all levels, extending to about 150°E above ~35 km. Maxima in lamination in the lower stratosphere near 90°–150°E and 210°–270°E are associated with the main regions where tropical air is drawn up around the developing vortex. Continuous filamentation associated with the developing vortex and anticyclone in early November 1994 shows that transport and mixing processes previously reported during winter are already important during fall.

1. Introduction

The Atmospheric Trace Molecule Spectroscopy (ATMOS) instrument observations of Northern Hemisphere (NH) middle and low latitudes during the Atmospheric Laboratory for Applications and Science 3 (ATLAS 3) mission in early November 1994 [*Gunson et al.*, 1996] constitute a unique data set during NH fall. This data set, comprising profiles of ~30 species, includes simultaneous observations of a number of long-lived gases; profiles for many species extend from the upper troposphere through the stratosphere and mesosphere. Individual ATMOS profiles observed in the NH during ATLAS 3 often show complex vertical structure with local minima and/or maxima that may appear in a number of trace species measured simultaneously. While in some cases relatively large vertical scale features can be explained by profiles crossing the vortex edge, or by observations in tongues of subtropical air drawn up from low latitudes (both conditions indicated by examination of low-resolution potential vorticity (PV) maps), there is no immediate explanation for the origin of many of these features and in many cases no direct evidence from which to determine whether they are spurious or represent real atmospheric features.

Numerous modeling studies have shown the formation of small horizontal scale features around the polar vortex edge and in the anticyclone (the "Aleutian high") in the Arctic winter stratosphere through differential advection by the large-scale winds [e.g., *Pierce and Fairlie*, 1993; *Waugh et al.*, 1994; *Sutton et al.*, 1994; *Mariotti et al.*, 1997; *Harvey et al.*, 1999, and references therein]. *Orsolini* [1995] and *Schoeberl and Newman* [1995] showed that deep filaments that tilt with height may lead to lamination in idealized tracers. A few recent studies using observed trace-gas fields for model initialization have shown that laminae with a wide range of vertical scales can result from filaments drawn off the vortex or from filaments drawn up from low latitudes and that such laminae are observed in trace-gas profiles [e.g., *Orsolini et al.*, 1997, 1998; *Manney et al.*, 1998].

Previous studies focused on the Arctic winter and spring (December through March), after the polar vortex was fully developed; none of the detailed studies using observed trace-gas fields for initialization and/or comparison with model results examined filamentation during fall, when the stratospheric polar vortex is in the process of developing. How-

[1]Jet Propulsion Laboratory, California Institute of Technology, Pasadena.

[2]Also at Department of Physics, New Mexico Highlands University, Las Vegas, New Mexico.

[3]Sandia National Laboratories, Livermore, California.

[4]Lockheed Martin Advanced Technology Center, Palo Alto, California.

Copyright 2000 by the American Geophysical Union.

Paper number 2000JD900428.
0148-0227/00/2000JD900428$09.00

ever, *Appenzeller and Holton* [1997] showed in a theoretical study that tracer lamination is expected in the entire "winter half-year," and *Manney et al.* [1996] showed that filaments formed in calculated high-resolution idealized tracer fields in November 1994 around the developing polar vortex (the "protovortex"), which was well defined above ~600 K. *Pierce and Grant* [1998] showed that rates of ozone lamination due to large-scale isentropic motions in the lower stratosphere at a NH midlatitude site began to increase starting in late October/early November. Seasonally averaged lamination rates in a high-resolution transport model also showed an increase in fall [*Orsolini and Grant*, 2000]. Wave activity and Rossby wave breaking, which are associated with filamentation, begin to increase between late October and late November, depending on the year [e.g., *Baldwin and Holton*, 1988]. A pattern reminiscent of the Aleutian high often begins to form in late October or early November [*Juckes and O'Neill*, 1988; *Rosier et al.*, 1994; *Harvey and Hitchman*, 1996], although it remains transient and is usually weak until late December. Several studies have shown low-latitude air being drawn up around the vortex and thick tongues drawn off the vortex in December [e.g., *Juckes and O'Neill*, 1988; *Harvey et al.*, 1999]; this process is thought to contribute to the formation of the main vortex/surf zone structure [e.g., *Juckes and O'Neill*, 1988] by strengthening potential vorticity and tracer gradients both along the vortex edge and in the subtropics. *Michelsen et al.* [1998a, 1998b] showed correlations of ATMOS NO_y, O_3, and CH_4 with N_2O that indicated some observations around the 1994 Arctic protovortex were influenced by subtropical air, confirming that air was drawn up from low latitudes.

The documented increase in wave activity and asymmetry of the developing vortex as early as late October makes lamination due to chaotic advection by the large-scale winds a plausible explanation for much of the structure seen in ATMOS long-lived trace-gas observations. *Manney et al.* [1999] showed that the ATLAS 3 ATMOS data provided good coverage of a wide range of dynamically distinct regions in the fall (northern) hemisphere, from the tropics to inside the protovortex. This relatively complete coverage in equivalent latitude/potential temperature space makes it possible to use ATMOS long-lived tracer fields to initialize high-resolution transport calculations. A reverse trajectory model [*Manney et al.*, 1998] is used to simulate high-resolution tracer profiles and maps during ATLAS 3. These calculations, and changes in ATMOS tracer-tracer correlations for individual profiles, show that many previously unexplained laminae in the observed profiles arose from small horizontal scale filaments sampled by ATMOS. Our analyses also illustrate the patterns of transport around the developing polar vortex during fall.

2. Data and Analysis

ATMOS version 3 data cover altitudes ranging from ~6 to 80 km. ATMOS spectra are recorded with a vertical spacing of ~2 km in the lower stratosphere to ~4 km in the upper stratosphere; this vertical spacing, combined with the instrument field of view, typically leads to an effective vertical resolution of ~2-6 km [*Gunson et al.*, 1996], with better resolution in the lower stratosphere than in the upper stratosphere. Strong features with vertical scales somewhat smaller than the ATMOS resolution may sometimes be detected, but the ATMOS retrievals would result in a broadened and smoothed version of such features. For each occultation during ATLAS 3, the signal-to-noise ratio was optimized by the use of one of a set of four optical bandpass filters (numbered 3, 4, 9, and 12); N_2O, CH_4, and H_2O were measured in all filters. The ATLAS 3 data were taken during November 3–12, 1994, and the sunset observations covered ~4°–50°N latitudes. *Gunson et al.* [1996] summarize the spatial coverage, filters used, and expected precision for each species. The recently produced version 3 ATMOS data set shows a number of improvements over version 2, particularly in the upper troposphere and lower stratosphere. Consistencies between tracers and tracer relationships are improved, and agreement between filters and with correlative data is better in many instances (F. W. Irion et al., The Atmospheric Trace Molecule Spectroscopy Experiment (ATMOS) version 3 data retrievals, manuscript in preparation, 2000; hereinafter referred to as manuscript in preparation; H. A. Michelsen et al., ATMOS version 3 water vapor measurements: Comparisons with ATMOS version 2 retrievals and observations from two ER-2 Lyman-α hygrometers, MkIV, MAS, HALOE, and MLS, submitted to *Journal of Geophysical Research*, 2000; hereinafter referred to as submitted manuscript). The precision of version 3 ATMOS N_2O and CH_4 is typically 5-10%, and that of H_2O 8-12% [*Michelsen et al.*, 2000; F. W. Irion et al., manuscript in preparation, 2000]. Temperatures are also retrieved from ATMOS observations in filters 3, 9, and 12, for altitudes from ~20 to 60 km [*Stiller et al.*, 1995]. The version 3 ATMOS data include separate estimates of the latitude and longitude of the observation at each altitude for which data are reported; these values may vary by as much as 5°–10° between the bottom and top of some profiles, although most vary by only a degree or two.

The methods used to simulate high-resolution maps and profiles at the ATMOS observation locations follow *Manney et al.* [1998]. Once-daily horizontal winds and temperatures from the Meteorological Office (UKMO) data [*Swinbank and O'Neill*, 1994] are used to drive the trajectory code described by *Manney et al.* [1994]; since the three-dimensional (3D) version of the trajectory code is used, the calculations include an estimate of diabatic descent. UKMO data are on a vertical grid with 2.5- to 3-km resolution; the actual vertical resolution is expected to be poorer, since the resolution of most data used in the assimilation is much worse. High-resolution trace-gas profiles and maps are obtained using a variation of the reverse trajectory (RT) technique developed by *Sutton et al.* [1994], as described by *Manney et al.* [1998]. High-resolution profiles are obtained on 100 isentropic (constant potential temperature, θ) surfaces equally spaced in log-θ between 380 and 2000 K (between ~13-16 and 50-55 km), giving a vertical spacing of ~350-400 m, about 6 times better than the vertical resolution of ATMOS. Since

ATMOS observations are at slightly different positions at each level, the ATMOS latitudes and longitudes are interpolated to the model θ levels to determine the central locations. An 11 × 11 array of parcels centered around these locations is placed in a 2° longitude × 1° latitude box (~100 km per side at midlatitudes) at each level. The profiles shown below are constructed from the average of the 121 parcels at each level; comparisons with profiles reconstructed from individual parcels verify consistency in the motions over the area of the column of initialized parcels [*Manney et al.*, 1998]. High-resolution maps are made on selected isentropic surfaces (chosen from the 100 levels on which the RT profiles are constructed) on an ~80 × 80 km equal area grid, interpolated to 0.8° latitude × 1.8° longitude for plotting. All RT calculations are for 7–8 days, with the trajectory calculations initialized at the nearest half hour (the trajectory time step) to the ATMOS observation time. Sensitivity tests discussed by *Manney et al.* [1998] showed that this time interval is sufficient to capture laminae of vertical extent greater than ~1 km. Since the model has previously been shown to reproduce laminae at this scale, we retain this resolution in the model to examine its predictions for scales smaller than those that can be verified using ATMOS data.

Initialization data are obtained from the ATMOS ATLAS 3 data mapped into equivalent-latitude/θ space [*Manney et al.*, 1999], reconstructed using PV calculated from UKMO data for the initialization day (the ending or earliest day of the back-trajectory calculations). PV calculated from the UKMO data is given on a 4° latitude × 5° longitude grid, on isentropic surfaces with spacing similar to the UKMO vertical (pressure) grid. Meteorological conditions in the NH during ATLAS 3 were such that ATMOS observations covered approximately 0°–60° equivalent latitude [*Manney et al.*, 1999]. With this coverage, RT tracer maps that fully cover the region outside and just inside the protovortex can be produced. Also, most of the air at the locations sampled by ATMOS was advected from regions (in equivalent latitude) also sampled by ATMOS, thus giving a complete or nearly complete simulated high-resolution vertical profile for most ATMOS observation locations. Since the initialization data are derived from the ATMOS data themselves, overall agreement between the large-scale structure of the calculated and observed profiles is expected. However, since the equivalent-latitude/θ fields involve averaging many observations (typically ~15–45 ATMOS-observed points in each PV/θ bin [*Manney et al.*, 1999]), they are highly smoothed; the PV used for reconstruction also varies significantly from day to day. Profiles reconstructed directly from ATMOS equivalent-latitude/θ fields thus show only those features with horizontal and vertical dimensions, and time persistence, large enough to be captured in the UKMO PV fields. By using these fields to initialize high-resolution transport calculations, we can estimate what smaller-scale and/or shorter-lived structures may be produced via advection by the large-scale winds.

To check the robustness of specific features in the simulated profiles, we have also constructed RT profiles of N_2O, CH_4, and H_2O using Upper Atmosphere Research Satellite (UARS) based "climatologies" [*Manney et al.*, 1999] constructed from Cryogenic Limb Array Etalon Spectrometer (CLAES) N_2O and CH_4 [*Roche et al.*, 1996] (using the recent version 9 data) and Microwave Limb Sounder (MLS) H_2O (prototype version 104) [*Pumphrey*, 1999] data. There are known biases between CLAES or MLS and ATMOS data [e.g., *Roche et al.*, 1996; *Pumphrey*, 1999; H. A. Michelsen et al., submitted manuscript, 2000]. However, if structure not apparent in the low resolution reconstructions appears in RT calculations initialized with the UARS-based climatologies as well as those initialized with ATMOS-derived fields, it provides verification that those structures result from advection of the large-scale tracer fields and not from irregularities in the ATMOS data. CLAES climatologies in NH midlatitudes at this time of year are reliable only down to ~500 K.

Manney et al. [1998] showed that the RT model usually reproduced laminae along the vortex edge (caused by vortex edge crossing or intrusions into the vortex) and outside the vortex (caused by filaments drawn off the vortex or up from low latitudes) when initialized with fields reconstructed from PV/θ space fields; best agreement was obtained for laminae arising from filamentation. This type of initialization should thus be appropriate for the study of lamination in midlatitudes and around the protovortex edge.

3. Results

3.1. Case Studies

We show here examples of laminae in ATMOS observations compared with results from the RT model described above. The four examples shown are chosen to illustrate laminae arising from low-latitude material drawn up around the protovortex, from material drawn off the vortex, and from varying vertical structure in the vortex edge region. There are also examples ranging from very good to poor agreement between model and observations.

Figure 1 shows N_2O, CH_4, and H_2O from ATMOS profile SS40, with corresponding calculated profiles. SS40 N_2O and CH_4 show a minimum/maximum pair at ~600–710 K and another (most obvious in CH_4) in the upper stratosphere at ~1100–1430 K. Although individual ATMOS H_2O profiles frequently contain some spurious wave-like structure [e.g., *Abbas et al.*, 1996], there are minima and maxima in SS40 H_2O that are anticorrelated with those in N_2O and CH_4. Since H_2O is a product of CH_4 oxidation, and older, photochemically aged air depleted in CH_4 is enriched in H_2O, H_2O and CH_4 are expected to be anticorrelated; this observation suggests that the features observed are of atmospheric origin. Neither pair of laminae is apparent in the profiles reconstructed from low-resolution data (reconstructed (RC) profiles, thick dashed and thin shaded dashed lines), except for a slight minimum in CH_4 near 1100 K. The ATMOS-RT calculations (thick solid lines), however, show very good agreement with the lower pair of laminae in N_2O and CH_4 and fairly good agreement with those in H_2O; the CLAES (N_2O and CH_4) and MLS (H_2O) based RT calculations (thin shaded lines) show corresponding minima and

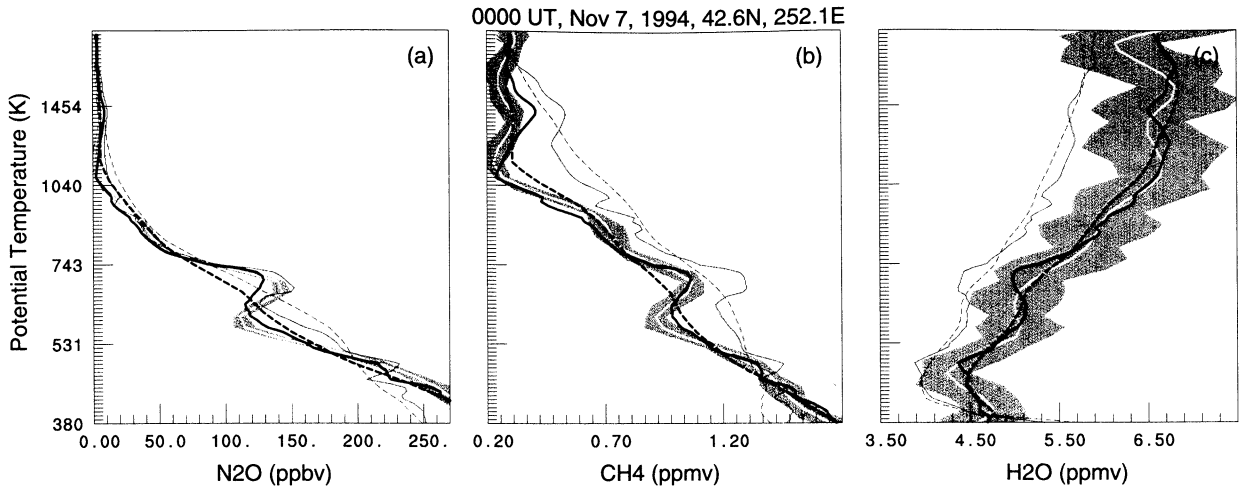

Figure 1. (a) N_2O (ppbv), (b) CH_4 (ppmv), and (c) H_2O (ppmv) mixing ratios for Atmospheric Trace Molecule Spectroscopy (ATMOS) profile SS40, on November 6, 1994. The white lines show the ATMOS observed values, with the surrounding shading indicating the estimated random error of the retrieval. The thick dashed lines show the low-resolution reconstructed (RC) profiles from the Meteorological Office (UKMO) potential vorticity (PV) and the ATMOS equivalent-latitude/θ tracer fields. The thick solid lines show the results of the reverse trajectory (RT) calculations initialized with the RC ATMOS data. The dashed and solid shaded lines show the RC and RT profiles using the UARS-based climatologies for tracer initialization (see text for details). The tick marks on the y axis are at the RT model levels.

maxima. The N_2O and CH_4 (H_2O) profiles from RT calculations show a distinct maximum (minimum) near 1430 K, similar to that in the ATMOS-observed profiles.

Plate 1 shows that in both the middle and upper stratosphere, SS40 observations were in the vicinity of a narrow tail of material pulled off the vortex edge. Near 1100 K (Plate 1b) the ATMOS observations were in a relatively wide portion of the tail, with very low CH_4 representative of air from well inside the protovortex. At 1430 K (Plate 1a) the tail drawn off the vortex was sheared out and folded back upon itself with higher CH_4 air from the vortex edge region; the SS40 observation was located along one of these filaments of higher CH_4. This maximum resulted from a filament too narrow to appear in the low-resolution tracer fields.

The tail drawn off the vortex was narrower at lower levels (Plates 1c and 1d), as seen in previous studies of the vertical structure of vortex filaments [e.g., *Schoeberl and Newman*, 1995]. Near 700 K, SS40 was in the cusp where the tail drawn off the vortex first curved around the developing anticyclone; here high CH_4 air drawn up from low latitudes was mixed into midlatitudes, resulting in moderately high CH_4 values. Near 600 K the ATMOS observation was in the filament of low CH_4 pulled off the vortex. Since neither this vortex filament nor the cusp region are well defined in the UKMO PV fields, the RC profiles show the CH_4 at both levels to have moderate values characteristic of air from the outside of the vortex edge region.

The ATMOS H_2O profile in Figure 1c shows an additional minimum in the lower stratosphere near 480 K (at this level, horizontal gradients in N_2O and CH_4 are relatively weak, so laminae would be small, and with the strong vertical gradients such smaller variations are not obvious). Although this minimum was apparent in the RC profiles, it is deeper and follows the ATMOS observations over more of its vertical extent in the RT profiles. At this time in the NH fall the lower stratospheric vortex is just developing [e.g., *Manney et al.*, 1999] and large-scale tracer gradients are relatively weak, but there is much stirring and filamentation in midlatitudes. Plate 2 shows that the SS40 observation was in a region where a broad filament of low-latitude, low-H_2O air had been drawn in and coiled up with high-H_2O air from the incipient vortex. This feature was enhanced by the seasonal cycle in tropical H_2O, since there was a minimum near this level in tropical profiles [e.g., *Abbas et al.*, 1996]. Even though the flow at this level is less organized than at higher levels, the region under the developing anticyclone can be readily identified as one of enhanced mixing in which fingers of low and high H_2O were folded together.

Figure 2 shows CH_4 profiles for ATMOS observation SS64. None of the laminae in the ATMOS-observed profile are apparent in the RC profiles. The RT profiles, however, show minima and maxima resembling those near 670–730 K and 460–515 K in the ATMOS profile, although there is a slight ($\sim$1 km) offset in the levels of the minimum near 730 K and the maximum near 520 K. In the upper stratosphere, although the RT profiles show some laminae that are not apparent in the ATMOS data, they follow the deep minimum in the ATMOS profiles much more closely than do the RC profiles.

Plate 3a shows that the deep minimum in the upper stratosphere results from a narrow filament drawn off the protovortex edge. The filament at 1170 K is the upward extension of a narrow filament seen at 731 K (Plate 3b), where the ATMOS

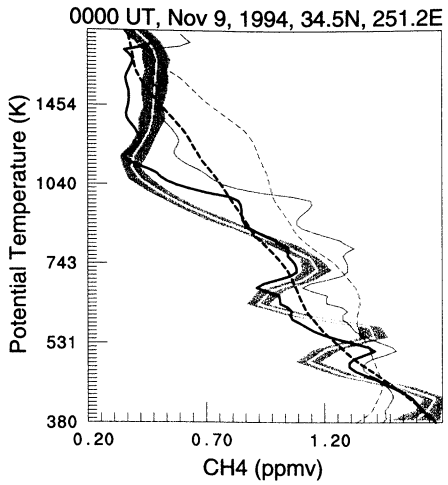

Figure 2. CH_4 (ppmv) mixing ratios for ATMOS profile SS64, on November 9, 1994. Layout and line styles are as in Figure 1.

observation was in a filament of midlatitude air with moderately high CH_4 drawn poleward of this vortex filament; near 670 K (not shown) the ATMOS observations were again in the vortex filament. The maximum at 514 K arose from a tongue of low-latitude, high-CH_4 air drawn up around the vortex edge, producing extremely strong tracer gradients (Plate 3c). Near 480 K (not shown) the observations were on the poleward side of this high-CH_4 tongue, giving rise to the minimum. *Manney et al.* [1998] showed examples where laminae were reproduced by RT calculations with small offsets in altitude, particularly in cases with extremely strong tracer gradients, as seen here, where a slight error in the position of a feature (e.g., the tongue of high-CH_4 air) could lead to a large difference in tracer values.

The SS07 ATMOS observations show an example of laminae forming when tropical air is drawn up around the vortex near 120°E, throughout the depth of the stratosphere (Figure 3 and Plate 4). In the RC profiles (thick dashed solid and thin dashed shaded lines), there is a shallow minimum/maximum near 600–700 K, indicating that the structure causing this feature is of large enough scale to appear in the averaged fields and/or the UKMO PV fields; this feature arises from the position of the vortex edge, such that observations near 600 K are poleward of the vortex edge, and near 700 K, equatorward of the vortex edge in a tongue of tropical air drawn up around the vortex. *Fairlie et al.* [1997] noted that high-resolution transport calculations such as these are useful for refining large-scale gradients along the vortex edge; this is apparent in the better representation of these laminae in the RT calculations. The RT-model profiles show a distinct minimum near 900 K, similar to that seen in the ATMOS observations, although the maximum above it in the ATMOS-RT profiles is not as large. Near 990 K the ATMOS observations were in a tongue of high CH_4 drawn up from low latitudes, whereas at 909 K (Plate 4) the observations were toward the inside of the vortex edge region, where CH_4 was lower. The RT calculations in this case indicate that the ATMOS observations near 900 K were farther into the vortex than suggested by the UKMO PV and were thus at lower CH_4 values. The smaller maximum in the ATMOS-RT profiles than in the observations near 1000 K may result from inaccuracies in the position of the filament of high CH_4 in the RT calculations: An RT map constructed using the CLAES-based initialization field shows the highest tracer region in the tongue extending farther poleward, resulting in the larger lamina near 1000 K in the CLAES-RT profile (Figure 3).

Laminae similar to those shown above are seen, and reproduced by the RT model, for many other ATMOS profiles in November 1994. There are also, however, cases where the RT calculations fail to reproduce laminar structure seen in ATMOS profiles and (as expected from the higher resolution of the RT model) cases where the RT model calculations produce laminae not observed by ATMOS. Figure 4 and Plate 5 show such examples for ATMOS profile SS23. Although there is a suggestion of a maximum near 600 K in the RC profiles (dashed solid and shaded lines, especially in the reconstruction from CLAES "climatology"), the RT profiles show little indication of the large maximum seen in the ATMOS observations. The lamina in the ATMOS data is robust, with a similar feature in N_2O and an anticorrelated feature in H_2O. Plate 5b shows that at 608 K, a large tongue of low-latitude air was drawn up around the vortex edge, which extended in a tail out to nearly 30°N, similar to the situation seen at lower levels for SS64 (Plate 3). This tongue extended from below 500 K to about 750 K, and the RT calculations show SS23 to be poleward of it at all levels. Given the apparent consistency between species, it is unlikely that the lamina in SS23 is a spurious feature in the ATMOS data; it is plausible that if uncertainties in the RT calculations resulted in a slightly calculated erroneous position or extent of the tongue of low-latitude air, ATMOS may have sampled air from this tropical tongue near 600 K. A misrepresentation of the calculated position of the tongue of low-latitude air could result

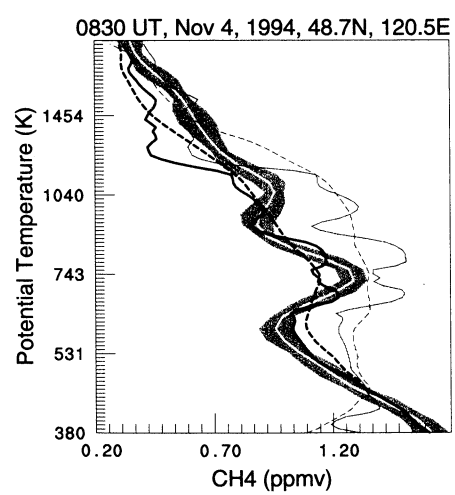

Figure 3. CH_4 (ppmv) mixing ratios for ATMOS profile SS07, on November 4, 1994. Layout and line styles are as in Figure 1.

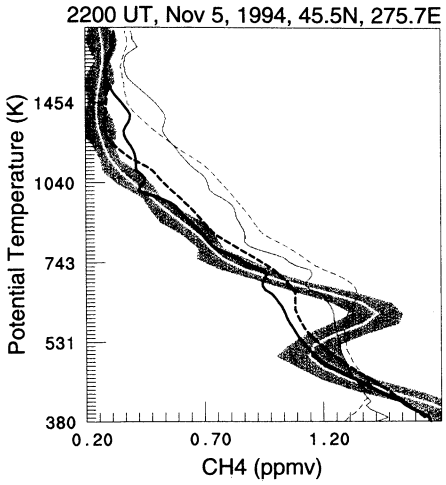

Figure 4. CH_4 (ppmv) mixing ratios for ATMOS profile SS23, on November 5, 1994. Layout and line styles are as in Figure 1.

either from inaccuracies in the winds or from advection of a feature that was inaccurately represented in the initialization fields reconstructed using UKMO PV.

Conversely, Plate 5a shows an example of a lamina in the RT model that does not show up in the ATMOS data. Several similar features are apparent in the upper stratosphere in Figures 2 and 3, where the RT model produces small laminae not seen by ATMOS. In each case, these features arise from very narrow filaments (either higher values mixed into the vortex edge region, as in Plate 5a, or low values drawn off the vortex). Since the ATMOS resolution is poorer in the upper stratosphere, extremely narrow filaments are more likely to be missed, especially if they are also vertically narrow (as is the one shown here) or tilt strongly with height. ATMOS does capture some such narrow features in the upper stratosphere (e.g., Figure 2 and Plate 3a), but detection of such features by ATMOS is likely to depend strongly on their exact location, tilt, and vertical extent.

While reproduction in the RT model of specific laminae, as shown above, provides a strong suggestion that those features are of atmospheric origin, the examples shown for SS23 illustrate the difficulty in definitively identifying an atmospheric origin of laminae from model calculations alone.

3.2. Tracer Correlations

The ability of the RT calculations to reproduce many individual laminae sampled by ATMOS suggests that these laminae are indeed of atmospheric origin and indicates the transport processes by which they arise. Correlations between N_2O and CH_4 provide further evidence for, and information about, the atmospheric origins of the features observed. *Michelsen et al.* [1998a] (combining all ATMOS observations) demonstrated that N_2O and CH_4 during ATLAS 3 had distinct correlations in the tropics and midlatitudes. Plate 6 shows N_2O/CH_4 correlations for the four profiles examined above (section 3.1), with the regions of the laminae color-coded, along with the fits to the tropical and midlatitude correlations during ATLAS 3 [*Michelsen et al.*, 1998a].

Laminae in SS07 (Plate 6a), the lower lamina in SS64 (Plate 6d, purple), and the lamina near 600 K in SS23 (Plate 6b) were associated with air drawn up around the protovortex edge from the tropics. Consistent with this, the N_2O/CH_4 relationships measured within these laminae shift to the tropical correlation curve, whereas above and below each lamina the measured N_2O/CH_4 correlations follow the midlatitude curve. The transition of the SS23 correlation in the region of the lamina to the tropical curve strongly supports the suggestion above that this feature results from observations in the tongue of tropical air drawn up around the protovortex tail. Below about 460 K (above ~280-300 ppbv of N_2O, where SS07 and SS23 show tropical correlations while SS64 suggests more midlatitude-like conditions), the vortex is not as well defined, the flow is more chaotic, and tracer gradients are weak; thus there is little differentiation between tropical and midlatitude air. The distances between the *Michelsen et al.* [1998a] curves in this region are within the uncertainties for individual profiles (which increase below about 400 K).

The upper lamina discussed for SS40 is at an altitude where N_2O and CH_4 mixing ratios are sufficiently low that it is difficult to distinguish between tropical, midlatitude, and protovortex air (Plate 6c, green segment); insofar as one can tell, the correlation for this lamina does appear to fall on the midlatitude curve, which would be expected, since Plate 1a showed the higher CH_4 filament to have values characteristic of the protovortex edge region.

The lower lamina in SS40 (Plate 6c, purple segment) and the lamina in SS64 in the 650- to 750-K region (Plate 6d, green) had maxima with moderately high, midlatitude CH_4 values and minima in vortex filaments. While the maxima fall along the midlatitude curve, the minima actually fall significantly below that curve, suggesting a separation of the protovortex correlation from the nominal midlatitude relationship. *Michelsen et al.* [1998a] showed that in NH spring, the vortex N_2O/CH_4 correlation from ~20 to 250 ppbv of N_2O fell approximately along a line connecting those points on the midlatitude curve, as a result of descent in the vortex and mixing with extravortex air. *Plumb et al.* [2000] showed that this curve in fact results from descent and mixing that take place throughout the winter. Consistent with this conclusion, the separation of the protovortex correlation from the midlatitude correlations indicates that at levels above ~600–700 K, enough descent in the vortex and mixing with midlatitude air have already occurred in early November to change the N_2O/CH_4 relationship in protovortex air. This result was not obvious in the work by *Michelsen et al.* [1998a] since the collection of all protovortex observations did not separate those near the protovortex edge from those well within the protovortex, because profiles of apparently "mixed" origin (including some of those shown here) were excluded from the analyses and because the tracer relationships for individual ATMOS profiles in version 2 data did not show this behavior clearly. A change in the vortex

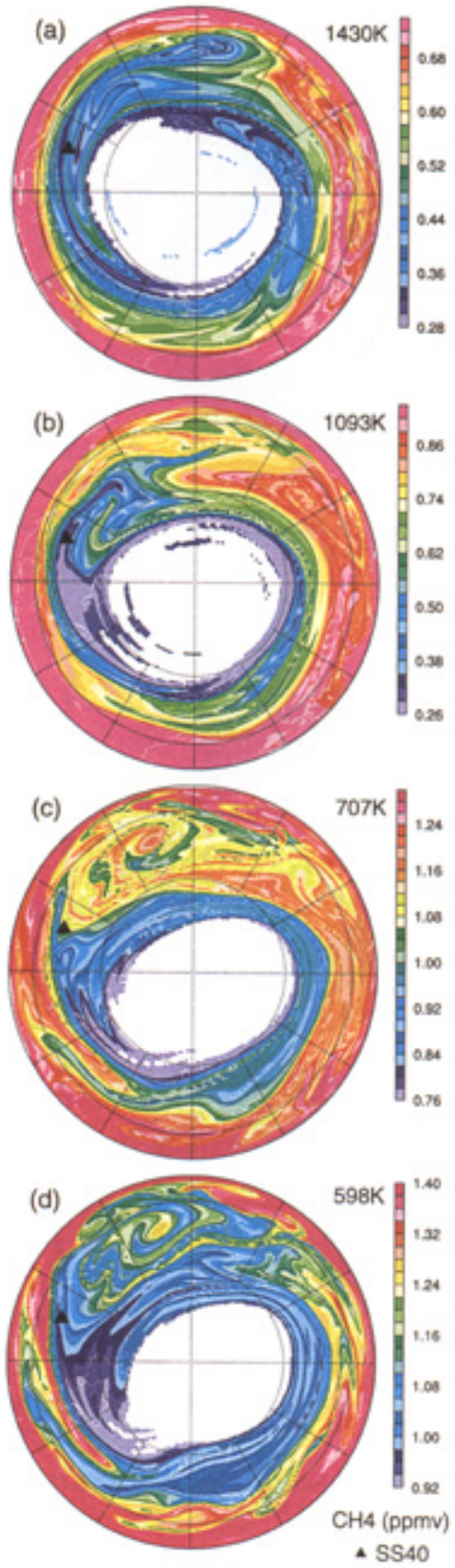

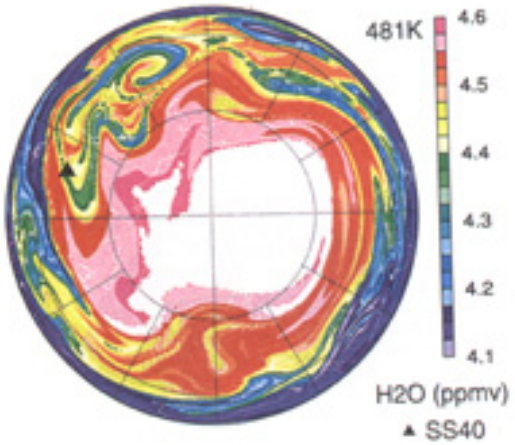

Plate 2. Same as in Plate 1, but for RT H_2O at 481 K.

Plate 1. High-resolution NH maps of CH_4 from RT calculations initialized with ATMOS equivalent-latitude/θ fields (see text) for 0000 UT, November 7, 1994, near the observation time of SS40. Levels shown are (a) 1430 K, (b) 1093 K, (c) 707 K, and (d) 598 K. The black triangle indicates the position of SS40. The map projection is orthographic, with 0° longitude at the bottom and 90°E to the right. The domain is from equator to pole, with thin dashed lines at 30 and 60°N. Note that the contour interval is different at different levels, to emphasize the horizontal structure in the fields.

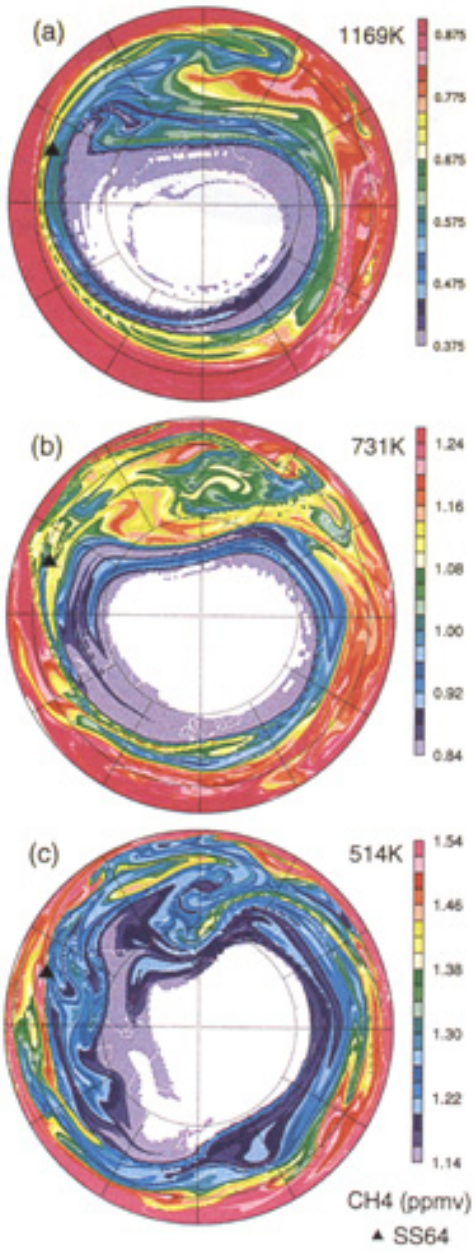

Plate 3. Same as in Plate 1, but for SS64, 0000 UT, November 9, 1994. Levels shown are (a) 1169 K, (b) 731 K, and (c) 514 K.

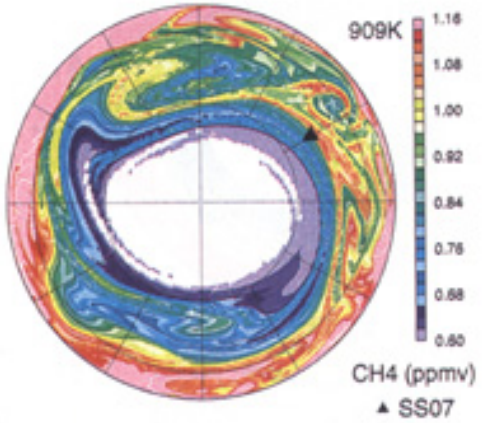

Plate 4. Same as in Plate 1, but for SS07, 0830 UT, November 4, 1994, at 909 K.

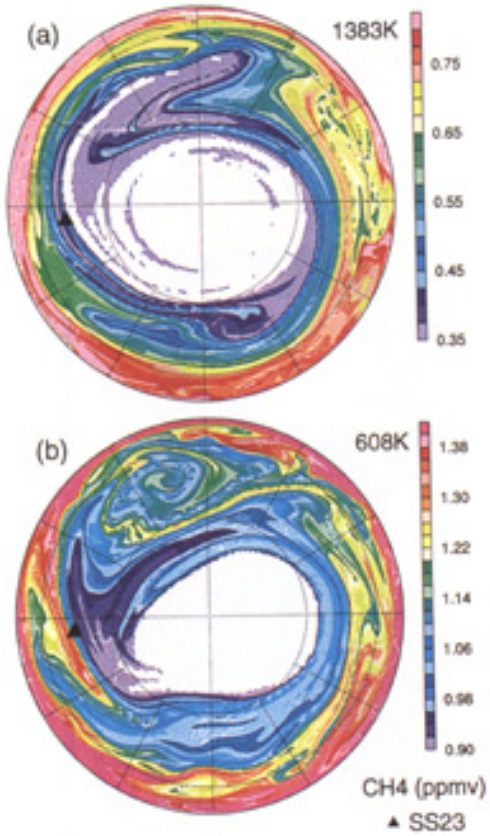

Plate 5. Same as in Plate 1, but for SS23, 2200 UT, November 5, 1994, at (a) 1383 K and (b) 608 K.

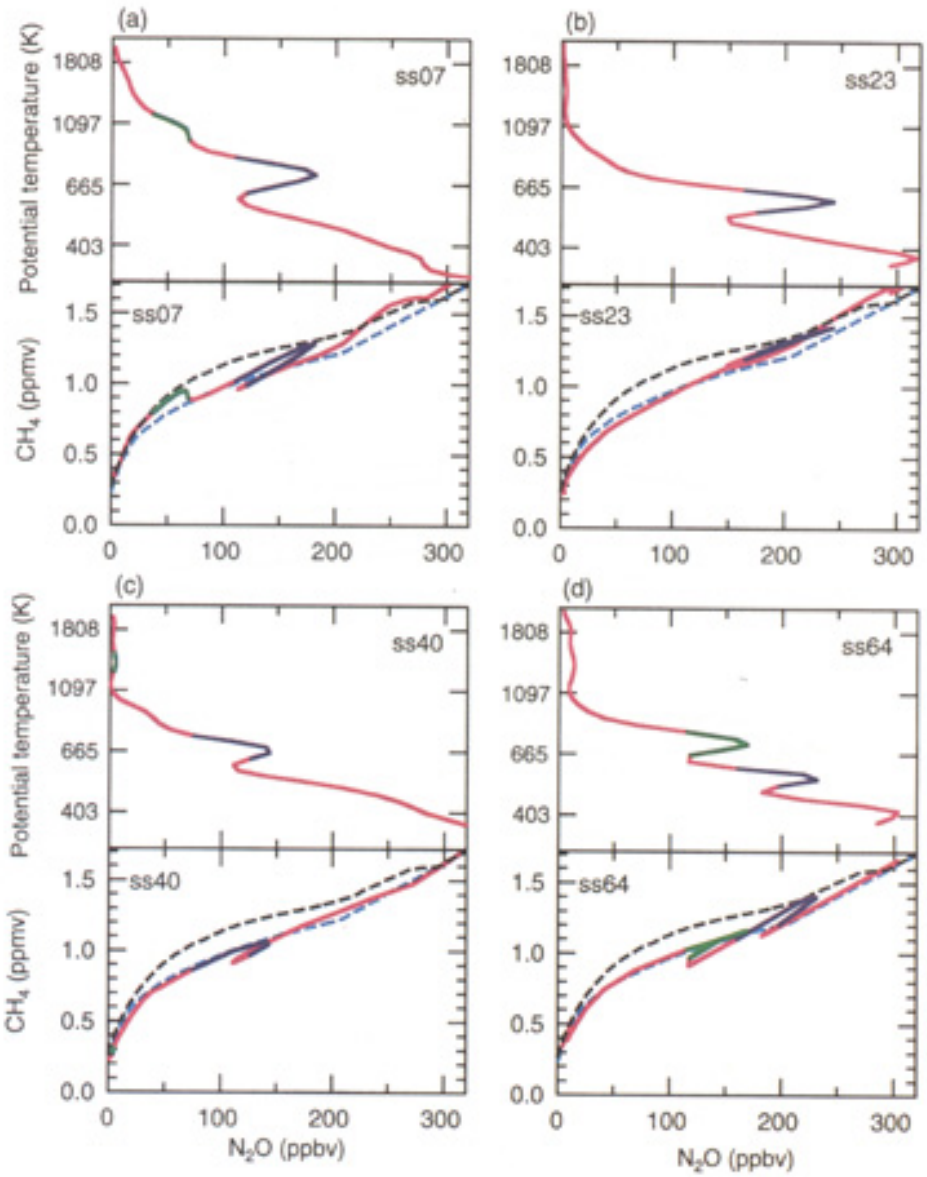

Plate 6. N_2O/CH_4 correlations for (a) SS07, (b) SS23, (c) SS40, and (d) SS64. Top panel in each plot shows the N_2O profile, with the regions of laminae color-coded (purple for lower lamina maximum and, in Plates 6a, 6c, and 6d, green for upper lamina maximum). Bottom panel shows the correlation for that profile with the same color coding. The dashed black line in each of the bottom panels shows the tropical correlation curve derived by *Michelsen et al.* [1998a], and the dashed cyan line shows the corresponding midlatitude curve.

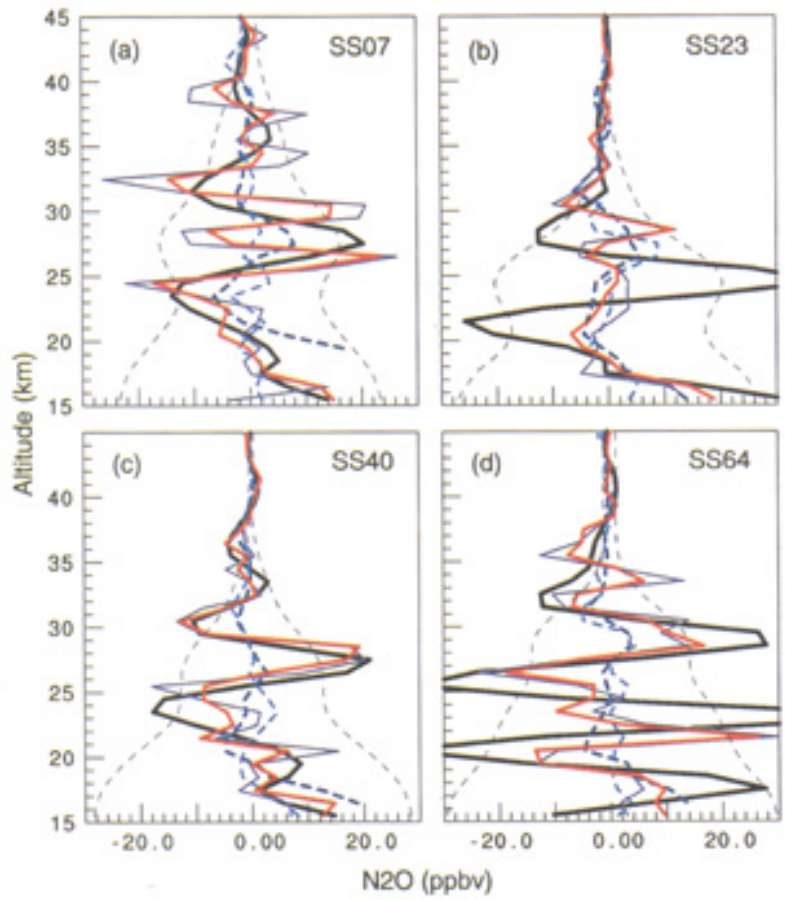

Plate 7. N_2O perturbation profiles for (a) SS07, (b) SS23, (c) SS40, and (d) SS64 with a five-point running mean smoothed profile (on ATMOS 1-km grid) removed. Bold solid black lines show ATMOS profile, dashed blue lines show ATMOS-RC profiles, dashed cyan lines show Cryogenic Limb Array Etalon Spectrometer (CLAES)-RC profiles, solid red lines show ATMOS-RT profiles, and solid purple lines show CLAES-RT profiles. Thin dashed grey lines show deviations of 10% from the original ATMOS profile.

N_2O/CH_4 correlation such as that seen here requires that for some time, the vortex has been substantially, but not completely, isolated, so that mixing across the vortex edge is weak or sporadic [*Plumb et al.*, 2000]. Thus the observed changes in the correlations demonstrate that there has been relatively confined descent in the vortex for some time, accompanied by weak or sporadic mixing with extravortex air.

3.3. Laminae Statistics and Distributions

3.3.1. Laminae counts and statistics. To characterize more generally the performance of the RT model, statistics of RT model skill (following *Manney et al.* [1998]) and laminae counts (following, e.g., *Pierce and Grant* [1998]) were done for all ATMOS observation locations north of 30°N (67 ATMOS profiles), for CH_4 and N_2O. Individual ATMOS H_2O profiles contain too many spurious variations (H. A. Michelsen et al., submitted manuscript, 2000) to make such calculations informative. These counts and statistics are compared with those for low-resolution reconstructed (RC) profiles, to assess whether the RT calculations show better overall agreement with ATMOS than the RC profiles.

Perturbation profiles for use in counting and statistical analysis were obtained following *Pierce and Grant* [1998]. For each profile, on the ATMOS (1 km) grid (RC and RT profiles linearly interpolated), a five-point boxcar running mean was taken to obtain a "smoothed" profile with local variations (individual minima or maxima less than 5 km deep) removed. A perturbation profile was obtained by subtracting the smoothed profile from the original profile. Plate 7 shows examples of N_2O perturbation profiles for the four cases in section 3.1. Plate 7d, for example, shows clearly how well the features in SS64 agree with those in the RT models and demonstrates that in the lower stratosphere, the apparent disagreement consists mainly of a ~1-2 km altitude offset in the lamina near 21 km. SS40 (Plate 7c) shows good agreement between ATMOS and RT profiles over most of the vertical range, but the deep lamina in the ATMOS profile centered near 23 km is modeled as two laminae (near 22 and 25 km). SS07 (Plate 7a) shows similar "split" laminae

near 28 and 35 km. These split laminae could be features that ATMOS does not fully resolve.

Applying a similar procedure to get perturbation profiles of θ (derived from the ATMOS temperatures) for profiles from filters 3, 9, and 12, following *Pierce and Grant* [1998] and *Teitelbaum et al.* [1996], shows no evidence for θ perturbations that are correlated with the trace- gas perturbations in midlatitudes. The laminae in ATMOS profiles are thus unlikely to be attributable to gravity wave variations [e.g., *Pierce and Grant*, 1998]. This does not imply that no gravity wave perturbations are present, as the limited vertical resolution of ATMOS precludes detection of many gravity wave features, which typically show multiple individual laminae that are each 0.5-2 km deep [e.g., *Teitelbaum et al.*, 1996, and references therein].

Manney et al. [1998] examined the skill of RT ozone calculations using correlation coefficients and Kolmogorov-Smirnov (KS) statistics, a procedure similar to that used by *Fairlie et al.* [1997]. The KS significance [e.g., *Gibbons*, 1985] compares frequency distributions; thus it is not affected by possible altitude offsets between observed and modeled profiles, as is the correlation coefficient. A similar procedure was used here. Correlation coefficients and KS significance were calculated between each ATMOS N_2O and CH_4 profile and the corresponding RC and RT profiles. Correlation coefficients and KS significance between ATMOS and RC profiles are referred to hereinafter as R_{RC} and KS_{RC}, respectively, and those between ATMOS and RT profiles are referred to as R_{RT} and KS_{RT}, respectively. Higher R_{RT} and/or KS_{RT} than R_{RC} and KS_{RC} indicates better RT model skill in reproducing structure in ATMOS profiles. These statistics were calculated both for the actual mixing ratio profiles and for the perturbation profiles described above. Statistical analyses were done from 15 to 45 km; dividing the range into upper and lower sections indicated no significant difference in skill between the upper and lower stratosphere. Statistics are done only up to 45 km, since above that level N_2O and CH_4 mixing ratios are so low that insignificantly small variations may be counted as laminae, and because of poorer ATMOS vertical resolution in the upper stratosphere, fewer variations in atmospheric structure due to thin filaments are likely to have been detected.

Table 1. Statistics of ATMOS/Calculated Profile Agreement for N_2O for Individual Profile Examples, From 15 to 45 km

Profile/ Statistic	Comparison of ATMOS Profile With Modeled Profiles			
	AT-RC	AT-RT	CL-RC	CL-RT
SS07				
R	-0.04	(0.47)	0.16	(0.21)
KS	0.32	(0.999)	0.15	(0.96)
SS23				
R	(0.38)	(0.49)	0.23	(0.40)
KS	(0.41)	(0.61)	(0.41)	(0.41)
SS40				
R	0.35	(0.73)	0.03	(0.65)
KS	0.24	(0.96)	0.25	(0.999)
SS64				
R	0.25	(0.40)	0.16	(0.41)
KS	0.07	(0.81)	0.08	(0.81)

Abbreviations are AT-RC, ATMOS reconstructed profile; AT-RT, reverse trajectory profile initialized with AT-RC; CL-RC, CLAES reconstructed profile; CL-RT, reverse trajectory profile initialized with CL-RC; R, correlation coefficient; KS, Kolmogorov-Smirnov significance. R values in parentheses are statistically significant at the 95% level. KS values in parentheses are greater than expected from a Monte Carlo test [*Manney et al.*, 1998].

Table 2. Average Statistics of ATMOS/Calculated Profile Agreement for 67 Profiles, From 15 to 45 km

Species/ Statistic	Comparison of ATMOS Profile With Modeled Profiles			
	AT-RC	AT-RT	CL-RC	CL-RT
N_2O				
R×100	49±22	39±21	26±24	16±21
KS×100	42±24	71±27	32±26	69±27
%R+	–	25%	–	36%
%KS+	–	82%	–	81%
CH_4				
R×100	43±21	26±18	08±26	08±18
KS×100	19±17	65±27	25±22	64±29
%R+	–	19%	–	46%
%KS+	–	91%	–	82%

Abbreviations are %R+, percent of profiles with larger R for ATMOS and RT than for ATMOS and RC profiles; %KS+, percent of profiles with greater KS for ATMOS and RT than for ATMOS and RC profiles.

Since the RC and RT profiles use PV from the same source, and for the ATMOS RC and RT profiles, the trace-gas or initial fields are derived from averaged ATMOS data, good agreement between the large-scale structure in all the profiles considered here is expected. This agreement is reflected in the statistics for the actual trace-gas profiles, which yield very high (statistically significant, according to a Student's *t*-test) correlation coefficients between ATMOS and nearly all of the RC and RT profiles. *Manney et al.* [1998] showed that calculations for the complete (as opposed to perturbation) trace-gas profiles frequently show little increase in R_{RT} and KS_{RT} over R_{RC} and KS_{RC}; R_{RT} and KS_{RT} are larger than R_{RC} and KS_{RC} for 33-63% (depending on species and initialization type) of the profiles examined here.

Improvements in the representation of small-scale structure are more readily seen in the perturbation profiles, which have large-scale ($\gtrsim$5 km) structure removed [e.g., *Manney et al.*, 1998]. Table 1 summarizes statistical results for N_2O (similar results are obtained for CH_4) for the perturbation profiles shown in Plate 7. The results for SS07, SS40, and SS64 are typical of those for cases where prominent laminae in the ATMOS profiles were reproduced in the RT model. For the perturbation profiles, both R_{RT} and KS_{RT} are much larger than R_{RC} and KS_{RC}. R_{RT} values are statistically significant, whereas R_{RC} values are not; these are cases where the RT model produces specific laminae that are not present in the RC fields. In many cases, especially where there are not large laminae in the ATMOS profiles, the R_{RC} values are statistically significant, and R_{RT} values are often lower, with KS_{RT} typically only a little higher than KS_{RC} (similar results to those shown in Table 1 for SS23).

Table 2 summarizes the results of statistical calculations for the 67 perturbation profiles. As was the case for the ozone profiles modeled by *Manney et al.* [1998], R_{RT} values were on average lower than R_{RC} values, with only 20-50% of R_{RT} values higher. However, over 80% of the RT profiles show higher KS significance. As discussed by *Fairlie et al.* [1997] and *Manney et al.* [1998], the correlation coefficient can be misleading, as laminae that are otherwise well reproduced by the RT model often show small altitude offsets from those in the observations; such offsets may result in large decreases in the correlation coefficient. Since the KS statistic compares frequency distributions, it does not suffer from this sensitivity, and the larger values of KS_{RT} than KS_{RC} shown in Table 2 suggest that the RT model shows skill in reproducing laminae in ATMOS observations.

Another simple measure of closer agreement between RT model and ATMOS profiles than RC and ATMOS profiles, which helps to verify that laminae are being produced near the right altitude, is to compare the number of "matching" (i.e., the right profile, same sign, and approximately the same altitude or θ-level) laminae between ATMOS and RC profiles with those between ATMOS and RT profiles. Table 3 summarizes such counts for N_2O from the ATMOS-RC initialization on the RT-model θ-grid (similar results were obtained for CH_4 and for the ATMOS grid), divided into several vertical ranges. An N_2O perturbation greater than 10% of the mean profile value is identified as a lamina (dashed grey lines in Plate 7 show that cutoff for the ATMOS profile); all perturbations of the same sign at contiguous levels that satisfy this condition are counted as one lamina. (Because of the smaller vertical gradients, a different cutoff is appropriate for CH_4; a perturbation greater than 6% was used for that cutoff.) These conditions identify as laminae most features that were noted visually (e.g., those where the ATMOS profiles cross the grey lines in Plate 7), and few others, but occasionally undercount below 20 km, as seen in Plate 7c where the ATMOS lamina near 19 km does not cross the grey line. (However, conditions based on a mixing ratio value appropriate for the middle or lower stratosphere would much more severely undercount in the upper stratosphere.) To count on the model grid, the mean profiles were constructed using an 11-point mean, to again remove variations smaller than ~5 km.

Table 3. Laminae Counts for ATMOS, RC, and RT Model Profiles

θ Range, K	Number of Laminae		
	ATMOS	RC	RT
380 – 442	2	0	0
442 – 523	2	0	1
523 – 618	4	0	0
618 – 731	7	0	4
731 – 864	6	0	4
864 – 1022	14	1	7
1022 – 1209	22	2	18
1209 – 1430	20	2	17
Total (380 – 1430)	77	5	51

RC and RT counts are laminae from the ATMOS-RC and ATMOS initialized RT profiles that match in location (profile number, approximate θ level) and sign those in the ATMOS data.

Laminae corresponding to ~2/3 of those observed by ATMOS were counted in the RT model profiles, as opposed to only ~7% in the low-resolution reconstructions (RC profiles). Few of the laminae seen in ATMOS observations were counted in the model profiles below ~600 K. At the lowest levels, especially below about 550 K, the coverage of the equivalent latitude/θ ATMOS fields used for initialization is less complete [*Manney et al.*, 1999], resulting in several profiles with missing values at the bottom; 30 of the profiles do not have good values for all profiles down to the bottom of the range. Also, as noted above and seen in Plate 7, the criterion used may undercount at the lowest levels; several cases have been noted similar to that in Plate 7d, where (near 20 km) both ATMOS and the RT model produce laminae but the model lamina was not large enough to be counted (did not meet grey line). Although the correlation coefficients and KS statistics did not show a significant difference in agreement between the lower and upper stratosphere, it is also possible that because the vortex is less well developed below ~20 km (~600 K), with more vigorous mixing and filaments on smaller scales (e.g., Plate 2), the RT model here is more sensitive to small errors in the wind and PV fields and may mislocate filaments, as was the case for the lamina near 600 K in SS23 (section 3.1, Figure 4); this may occur even though the fields produced by the RT model still represent the type and distribution of structure present in the atmosphere.

3.3.2. Laminae distributions and dynamical implications. Figure 5 summarizes the patterns of N_2O laminae north of 30°N for three altitude regions and six longitude bins. Counts on the ATMOS grid are shown in order to accurately represent the laminae actually observed; the counts are normalized by the total number of ATMOS profiles in the longitude bin. Again, we see that the RT model is not very successful in reproducing laminae in the lower stratosphere (15–25 km); between 25 and 45 km, the patterns of lamination in the RT model generally resemble those in the ATMOS observations, with the most striking feature being a minimum in lamina occurrence in the 30°–90°E region, extending through the 90°–150°E region above 35 km. That the RT model produces more laminae than ATMOS in the middle and upper stratosphere (note that the scales are different in Figures 5a and 5b) is likely due primarily to the better RT model vertical resolution compared with ATMOS at higher levels (Figure 4 and Plate 5 showed an example of physically plausible laminae in the upper stratosphere that were not captured by ATMOS). In early November 1994, N_2O (Figure 5a) and CH_4 (not shown) laminae captured by ATMOS were more common in the middle to upper stratosphere than in the lower stratosphere. Although some laminae occur in all longitude bins (consistent with the prevalence of filaments seen in the RT maps), there is clustering, particularly in the lower stratosphere, where two large maxima in laminae occurrence are seen in the 90°–150°E and 210°–270°E bins and very few laminae are seen in the 330°–0°–30°E bin as well as in the 30°–90°E bin. At higher levels,

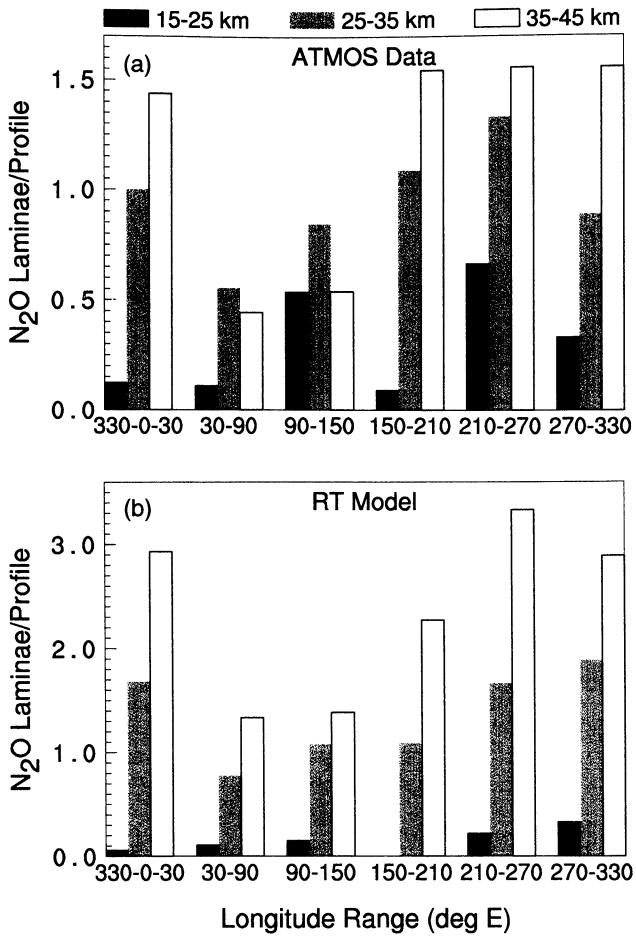

Figure 5. Distribution of N_2O laminae (a) observed by ATMOS and (b) from RT calculations at the ATMOS observation locations north of 30°N during ATLAS 3, in three altitude ranges and six longitude bins. RT calculations were interpolated to the ATMOS vertical grid before counting.

the minimum near 30°–90°E is the only pronounced feature.

Fewer laminae in the lower stratosphere compared to higher levels may result from several processes: (1) There may be less filamentation in the lower stratosphere when the polar vortex is less developed and planetary-scale wave activity is weaker than at higher levels; *Pierce and Grant* [1998] showed lower ozone lamination rates due to Rossby wave motions during October and November than during December and January in the lower stratosphere. (2) Fewer laminae may be detected by ATMOS in the lower stratosphere because of its limited vertical resolution, since both the horizontal and vertical scales of laminae tend to be smaller in the lower stratosphere [e.g., *Schoeberl and Newman*, 1995; *Bird et al.*, 1997]. (3) Fewer laminae may be seen in N_2O and CH_4 because their horizontal gradients are not as strong in the lower stratosphere in fall and early winter before descent has transported lower N_2O or CH_4 values in the vortex to these altitudes [e.g., *Manney et al.*, 1999].

The distribution of N_2O laminae observed by ATMOS in the lower stratosphere is qualitatively consistent with that shown by *Orsolini and Grant* [2000] in a multiyear transport model simulation. Their laminae distribution for September-October-November (SON) showed a relatively uniform band of high lamination rates in midlatitudes, with slight minima between ~20° and 60°E and between ~180° and 240°E. For December-January-February (DJF), their distribution was more localized, with a large maximum from ~90° to 210°E (in the Aleutian high region) and the deepest minimum between 30° and 90°E. The ATMOS lower stratospheric observations show more clustering than the model SON distributions but less than the model DJF distributions, with a maximum in the developing Aleutian high region and a deep minimum in the 30°–90°E region.

The 90°–150°E and 210°–270°E regions with lamination maxima in the lower stratosphere are in the main "entrance" regions, where air is drawn up from low latitudes around the protovortex, and the 210°–270°E region includes the area where material is coiling up in or folding up under the developing anticyclone. In the middle and upper stratosphere the tongues of material drawn up in the 90°–150°E region are coiling up with midlatitude air in the Aleutian high, and tongues of material drawn up around 210°–270°E stretch out to the 330°–0–30°E region and at times coil up in that region in a weaker anticyclone; additional tongues of low-latitude air are also drawn in from low latitudes farther east. As seen in the RT maps, the flow in the 30°–90°E region at all levels is more zonal, with less folding than seen at other longitudes, consistent with the minimum in lamination. Above ~35 km this relatively zonal flow extends farther east.

These distributions are consistent with the development of the vortex in early November 1994. The Arctic vortex in the middle and upper stratosphere (above ~600 K) is typically well established by early November [e.g., *Waugh and Randel*, 1999]. The presence of descent and some degree of confinement in the vortex in the middle and upper stratosphere (above ~800 K) during October and early November 1994 were shown by *Manney et al.* [1999]; that the vortex in the middle and upper stratosphere (above ~600 K) has been a major influence on transport at high latitudes for some time by early November 1994 was demonstrated by the change in N_2O/CH_4 correlations in vortex filaments (section 3.2). In early November 1994 a feature resembling the Aleutian high was present in the middle and upper stratosphere, consistent with the sometimes early appearance of this feature [*Harvey and Hitchman*, 1996] and the associated increase in wave activity [*Baldwin and Holton*, 1988]. The tongues of low-latitude air drawn up around the vortex and the tails of air drawn off the vortex are associated with this feature.

The Aleutian anticyclone was strongest in the middle stratosphere, between ~600 and 800 K (Plates 1c, 1d, 3b, and 5). At higher levels the protovortex was more symmetric, the Aleutian anticyclone was less pronounced, a second weaker anticyclone appeared near 0° longitude, and air from low latitudes was drawn up around the vortex in several regions in long, relatively zonal tongues (Plates 1a, 1b, 3a, and 4). This pattern, with the strongest anticyclone and largest displacement of the vortex from the pole in the middle stratosphere, resembles those reported during minor warmings in December [e.g., *Labitzke*, 1977; *Juckes and O'Neill*, 1988;

Rosier et al., 1994]. The appearance in early November 1994 of circulation patterns in the middle and upper stratosphere similar to those frequently reported for December demonstrates the early influence of the developing Aleutian high, strengthening vortex, and increasing wave activity and vortex asymmetry on tracer transport. The RT maps and ATMOS observations show that these processes are associated with substantial tracer lamination.

4. Summary and Conclusions

The veracity of laminar structures in ATMOS long-lived trace-gas profiles observed during the ATLAS 3 mission in early November 1994 has been tested using reverse trajectory (RT) calculations, tracer correlations, and laminae distributions; these methods are also used to identify the origins of specific laminae seen in ATMOS long-lived trace-gas observations. Laminae distributions were compared for observations and the RT model, and high-resolution maps and tracer correlations were used to illustrate the structure and evolution of the protovortex and long-lived tracers in fall 1994.

High-resolution profiles calculated using the RT model show that many long-lived trace-gas profiles observed by ATMOS in NH midlatitudes (~30°–50°N) during ATLAS 3 arose from filamentation due to chaotic advection by the large-scale winds. These features are often generated by sampling tropical air that is drawn up around the protovortex or filaments drawn out of the vortex. The first situation is confirmed by tracer-tracer correlations that move from typical midlatitude or protovortex to tropical correlations in the regions of laminae, indicating that the air sampled by ATMOS has the characteristics of tropical air in multiple simultaneously sampled species. When filaments from well within the vortex were sampled in the middle stratosphere, tracer correlations moved significantly below the canonical midlatitude correlation curve, indicating that enough confined descent accompanied by weak or sporadic mixing with extravortex air had already taken place by early November so as to alter the tracer correlations in the protovortex.

In a few cases, RT calculations failed to reproduce laminae that were robust features in the ATMOS observations. It was found in such cases that features in the RT maps could have produced laminae but were slightly offset from the position of the ATMOS observations and that ATMOS tracer-tracer correlations showed changes consistent with sampling of different air masses. Such failures are thus likely due to inaccuracies in the RT calculations, either in the winds or in the PV used to reconstruct the initialization fields.

Statistical analyses showed large average increases in Kolmogorov-Smirnov (KS) significance between ATMOS and RT profiles over that between ATMOS and the low-resolution equivalent-latitude/θ reconstruction (RC) fields used for initialization, suggesting that the RT model calculations do in fact produce profiles that agree better, in a quantifiable sense, with the ATMOS profiles. Counts of the laminae show that the RT model produces laminae corresponding to at least ~2/3 of those observed by ATMOS. ATMOS and RT model counts agree least well below ~20 km, where equivalent-latitude/θ coverage of the initialization data is worse, the counting procedure is less reliable, and filament positions may be more sensitive to details of the wind and PV fields used by the model.

Lagrangian techniques, such as those used here, are increasingly being used in validation-type studies [e.g., *Bacmeister et al.*, 1999; *Lu et al.*, 2000, and references therein]. Without accounting for transport processes, such as those discussed here, features in the ATMOS profiles attributable to laminae could have been identified as retrieval artifacts. Such a misinterpretation could lead to significant difficulties for data intercomparisons and validation studies, particularly for conditions where filamentation is common. For ATMOS, with relatively precise observations of multiple long-lived gases, the combined use of RT calculations and tracer correlations is a powerful tool for verifying structure in the observations. For instruments for which appropriate long-lived trace gases may not be available to examine correlations, techniques such as RT calculations may still be of material assistance in confirming the atmospheric origin of such structure.

The distribution of laminae sampled by ATMOS in midlatitudes shows a minimum in the number of N_2O and CH_4 laminae in the 30°–90°E region. In the lower stratosphere (15-25 km, ~400–650 K) the two regions with maxima in lamination, 90°–150°E and 210°–270°E, are the main entrance regions where low-latitude air is drawn up around the anticyclone. In the middle stratosphere (25-35 km), the minimum in the 30°–90°E region is the only striking feature, but at higher levels (35-45 km), this minimum extends eastward to ~150°E. These distributions agree well with the locations of filaments and small-scale structure in RT maps. These data and calculations provide a more detailed picture than has previously been presented of the patterns of transport around the developing vortex in fall. In early November 1994, low-latitude material was being continuously drawn up around the protovortex throughout the stratosphere. In the middle stratosphere, there was vigorous and continuous mixing of this low-latitude air with midlatitude air and tongues drawn off the protovortex in the anticyclone; folding together of protovortex and tropical air extended into the lower stratosphere where the vortex was not yet well defined. Tracer correlations showed that transport in and around the protovortex had been sufficiently influenced by confined descent and mixing by early November that vortex correlations were distinguishable from midlatitude correlations. The agreement between structure seen in the RT calculations and features observed by ATMOS confirms the picture of a very dynamic, variable, and highly structured protovortex in the NH fall and shows resulting filamentation in trace-gas observations throughout the stratosphere earlier in the season than previous studies.

Acknowledgments. We thank the ATMOS and CLAES instrument teams for their role in producing the data sets used here, especially H. C. Pumphrey for MLS H_2O data and J. B. Kumer and J. L. Mergenthaler for CLAES data, the Meteorological Of-

fice (especially R. Swinbank) for meteorological (UKMO) data, R. B. Pierce and M. L. Santee for helpful discussions, and two anonymous reviewers for their valuable comments. Work at the Jet Propulsion Laboratory, California Institute of Technology, and the Lockheed Martin Advanced Technology Center was done under contract with the National Aeronautics and Space Administration. H.A.M. was supported by the NASA Atmospheric Chemistry, Modeling, and Analysis Program (NAS1-98118).

References

Abbas, M. M., et al., Seasonal variations of water vapor in the lower stratosphere inferred from ATMOS/ATLAS-3 measurements of H_2O and CH_4, *Geophys. Res. Lett.*, *23*, 2401–2404, 1996.

Appenzeller, C., and J. R. Holton, Tracer lamination in the stratosphere: A global climatology, *J. Geophys. Res.*, *102*, 13,555–13,569, 1997.

Bacmeister, J. T., V. Kuell, D. Offermann, M. Riese, and J. W. Elkins, Intercomparison of satellite and aircraft observations of ozone, CFC-11, and NO_y using trajectory mapping, *J. Geophys. Res.*, *104*, 16,379–16,390, 1999.

Baldwin, M. P., and J. R. Holton, Climatology of the stratospheric polar vortex and planetary wave breaking, *J. Atmos. Sci.*, *45*, 1123–1142, 1988.

Bird, J. C., S. R. Pal, A. I. Carswell, D. P. Donovan, G. L. Manney, J. M. Harris, and O. Uchino, Observations of ozone structures in the arctic polar vortex, *J. Geophys. Res.*, *102*, 10,785–10,800, 1997.

Fairlie, T. D. A., R. B. Pierce, W. L. Grose, G. Lingenfelser, M. Loewenstein, and J. R. Podolske, Lagrangian forecasting during ASHOE/MAESA: Analysis of predictive skill for analyzed and reverse-domain-filled potential vorticity, *J. Geophys. Res.*, *102*, 13,169–13,182, 1997.

Gibbons, J. D., *Nonparametric Methods for Quantitative Analysis*, 2nd ed., Am. Sci., New York, 1985.

Gunson, M. R., et al., The Atmospheric Trace Molecule Spectroscopy (ATMOS) experiment: Deployment on the ATLAS Space Shuttle missions, *Geophys. Res. Lett.*, *23*, 2333–2336, 1996.

Harvey, V. L., and M. H. Hitchman, A climatology of the Aleutian high, *J. Atmos. Sci.*, *53*, 2088–2101, 1996.

Harvey, V. L., M. H. Hitchman, R. B. Pierce, and T. D. Fairlie, Tropical aerosol in the Aleutian high, *J. Geophys. Res.*, *104*, 6281–6290, 1999.

Juckes, M. N., and A. O'Neill, Early winter in the Northern Hemisphere, *Q. J. R. Meteorol. Soc.*, *114*, 1111–1125, 1988.

Labitzke, K., Interannual variability of the winter stratosphere in the Northern Hemisphere, *Mon. Weather Rev.*, *105*, 762–770, 1977.

Lu, C.-H., G. K. Yue, G. L. Manney, H. Jaeger, and V. A. Mohnen, Lagrangian approach for Stratospheric Aerosol and Gas Experiment (SAGE) II profile intercomparisons, *J. Geophys. Res.*, *105*, 4563–4572, 2000.

Manney, G. L., R. W. Zurek, A. O'Neill, and R. Swinbank, On the motion of air through the stratospheric polar vortex, *J. Atmos. Sci.*, *51*, 2973–2994, 1994.

Manney, G. L., R. Swinbank, and A. O'Neill, Stratospheric meteorological conditions for the 3–12 Nov 1994 ATMOS/ATLAS–3 measurements, *Geophys. Res. Lett.*, *23*, 2409–2412, 1996.

Manney, G. L., J. C. Bird, D. P. Donovan, T. J. Duck, J. A. Whiteway, S. R. Pal, and A. I. Carswell, Modeling ozone laminae in ground-based Arctic wintertime observations using trajectory calculations and satellite data, *J. Geophys. Res.*, *103*, 5797–5814, 1998.

Manney, G. L., H. A. Michelsen, M. L. Santee, M. R. Gunson, F. W. Irion, A. E. Roche, and N. J. Livesey, Polar vortex dynamics during spring and fall diagnosed using trace gas observations from the Atmospheric Trace Molecule Spectroscopy instrument, *J. Geophys. Res.*, *104*, 18,841–18,866, 1999.

Mariotti, A., M. Moustaoui, B. Legras, and H. Teitelbaum, Comparison between vertical ozone soundings and reconstructed potential vorticity maps by contour advection with surgery, *J. Geophys. Res.*, *102*, 6131–6142, 1997.

Michelsen, H. A., G. L. Manney, M. R. Gunson, C. P. Rinsland, and R. Zander, Correlations of stratospheric abundances of CH_4 and N_2O derived from ATMOS measurements, *Geophys. Res. Lett.*, *25*, 2777–2780, 1998a.

Michelsen, H. A., G. L. Manney, M. R. Gunson, and R. Zander, Correlations of stratospheric abundances of NO_y, O_3, N_2O, and CH_4 derived from ATMOS measurements, *J. Geophys. Res.*, *103*, 28,347–28,359, 1998b.

Michelsen, H. A., F. W. Irion, G. L. Manney, G. C. Toon, and M. R. Gunson, Features and trends in ATMOS version 3 stratospheric water vapor and methane measurements, *J. Geophys. Res.*, *105*, 22,713–22,724, 2000.

Orsolini, Y. J., On the formation of ozone laminae at the edge of the Arctic polar vortex, *Q. J. R. Meteorol. Soc.*, *121*, 1923–1941, 1995.

Orsolini, Y. J., and W. B. Grant, Seasonal formation of nitrous oxide laminae in the mid and low latitude stratosphere, *Geophys. Res. Lett.*, *27*, 1119–1122, 2000.

Orsolini, Y. J., G. Hansen, U. Hoppe, G. Manney, and K. Fricke, Dynamical modelling of wintertime lidar observations in the arctic: Ozone laminae, and ozone depletion, *Q. J. R. Meteorol. Soc.*, *123*, 785–800, 1997.

Orsolini, Y. J., G. L. Manney, A. Engel, J. Ovarlez, C. Claud, and L. Coy, Layering in stratospheric profiles of long-lived trace species: Balloon-borne observations and modeling, *J. Geophys. Res.*, *103*, 5815–5825, 1998.

Pierce, R. B., and T. D. A. Fairlie, Chaotic advection in the stratosphere: Implications for the dispersal of chemically perturbed air from the polar vortex, *J. Geophys. Res.*, *98*, 18,589–18,595, 1993.

Pierce, R. B., and W. B. Grant, Seasonal evolution of Rossby and gravity wave induced laminae in ozonesonde data obtained from Wallops Island, Virginia, *Geophys. Res. Lett.*, *25*, 1859–1862, 1998.

Plumb, R. A., D. W. Waugh, and M. P. Chipperfield, The effects of mixing on tracer relationships in the polar vortices, *J. Geophys. Res.*, *105*, 10,047–10,062, 2000.

Pumphrey, H. C., Validation of a new prototype water vapor retrieval for the UARS Microwave Limb Sounder, *J. Geophys. Res.*, *104*, 9399–9412, 1999.

Roche, A. E., et al., Validation of CH_4 and N_2O measurements by the Cryogenic Limb Array Etalon Spectrometer instrument on the Upper Atmosphere Research Satellite, *J. Geophys. Res.*, *101*, 9679–9710, 1996.

Rosier, S. M., B. N. Lawrence, D. G. Andrews, and F. W. Taylor, Dynamical evolution of the northern stratosphere in early winter 1991/92, as observed by the Improved Stratospheric and Mesospheric Sounder, *J. Atmos. Sci.*, *51*, 2783–2799, 1994.

Schoeberl, M. R., and P. A. Newman, A multiple-level trajectory analysis of vortex filaments, *J. Geophys. Res.*, *100*, 25,801–25,815, 1995.

Stiller, G. P., et al., Stratospheric and mesospheric pressure-temperature profiles from the rotational analysis of CO_2 lines of ATMOS/ATLAS-1 observations, *J. Geophys. Res.*, *100*, 3107–3117, 1995.

Sutton, R. T., H. MacLean, R. Swinbank, A. O'Neill, and F. W. Taylor, High-resolution stratospheric tracer fields estimated from satellite observations using Lagrangian trajectory calculations, *J. Atmos. Sci.*, *51*, 2995–3005, 1994.

Swinbank, R., and A. O'Neill, A stratosphere-troposphere data assimilation system, *Mon. Weather Rev.*, *122*, 686–702, 1994.

Teitelbaum, H., M. Moustaoui, J. Ovarlez, and H. Kelder, The role of atmospheric waves in the laminated structure of ozone profiles at high latitude, *Tellus, Ser. A, 48*, 442–455, 1996.

Waugh, D. W., and W. J. Randel, Climatology of Arctic and Antarctic polar vortices using elliptical diagnostics, *J. Atmos. Sci.*, *56*, 1594–1613, 1999.

Waugh, D. W., et al., Transport out of the lower stratospheric Arctic vortex by Rossby wave breaking, *J. Geophys. Res.*, *99*, 1071–1088, 1994.

M. R. Gunson, Jet Propulsion Laboratory, Mail Stop 169-237, Pasadena, CA 91109.

F. W. Irion and G. C. Toon, Jet Propulsion Laboratory, Mail Stop 183-601, Pasadena, CA 91109.

G. L. Manney, Department of Physics, New Mexico Highlands University, Las Vegas, NM 87701. (manney@mls.jpl.nasa.gov)

H. A. Michelsen, Sandia National Laboratories, MS 9055, P.O. Box 969, Livermore, CA 94551.

A. E. Roche, Lockheed Martin Advanced Technology Center, Org H1-11, Building 255, 3251 Hanover Street, Palo Alto, CA 94304.

(Received March 2, 2000; revised July 10, 2000; accepted July 13, 2000.)